NPFC-2022-SSC PS10-WP05 (Rev. 1)

Updated stock assessment of Pacific saury (*Cololabis saira*) in the Western North Pacific Ocean through 2021

Yun-Wei Chou[1], Jhen Hsu[1], Yi-Jay Chang[1], Chih-hao Hsieh[1], Wen-Bin Huang[2], Tung-Hsieh Chiang[3]

1. Institute of Oceanography, National Taiwan University

2. Department of Natural Resources and Environmental Studies, National Dong Hwa University

3. Overseas Fisheries Development Council of Chinese Taipei

Summary

This paper describes the updated stock assessment of the Pacific saury (*Cololabis saira*) in the Western North Pacific Ocean (WNPO) based on the guideline of the 2021 SSC PS09. The assessment consisted of applying the Bayesian state-space surplus production model for estimating the biomass from 1980 to 2022 with available catches from 1980 to 2021. Abundance indices available for WNPO Pacific saury consisted of standardized catch-per-unit-effort (CPUE) of stick-held dip net fisheries from Japan (1980 – 2021), Chinese Taipei (2001 – 2021), Russia (1994 – 2021), Korea (2001 – 2021), and China (2013 – 2021), joint CPUE index (1994 – 2021) and biomass survey from Japan (2003 – 2022). Two base case models were considered for the assessment outputs. The results of the base case models indicated that the estimated biomass had a similar trend over years. The ensemble time-series of biomass is estimated to have an increasing pattern since 2000 with two peaks in 2003 and 2005, after then dramatically decreased overtime and below B_{MSY} in 2009 – 2022. It should be noted that the models estimate the lowest biomass level in 2020 (median B_{2020}/B_{MSY} = 0.29, 80 percentile range 0.18 – 0.51) and following a slight increase in 2021 and 2022 (median B_{2021}/B_{MSY} = 0.33, 80 percentile range = 0.19 – 0.56; median B_{2022}/B_{MSY} = 0.45, 80 percentile range = 0.23 – 0.77). In the recent three years (2020 – 2022), the biomass was estimated below the B_{MSY} (median $B_{2020\text{-}2022}/B_{MSY}$ = 0.36, 80 percentile range = 0.22 – 0.60). A steady increase in fishing mortality is estimated to have occurred from 2004 to 2018, but a decreasing trend in fishing mortality was found from 2019 to 2021. The recent average fishing mortality is estimated to be above F_{MSY} (median $F_{2019\text{-}2021}/F_{MSY}$ = 1.21, 80 percentile range = 0.71 – 2.16) while the fishing mortality in 2021 is less than F_{MSY} (median F_{2021}/F_{MSY} = 0.75, 80 percentile range = 0.43 – 1.45). The ensemble MCMC results from the two base cases indicated that the 2021 stock status is likely within the yellow quadrant (Prob [$B_{2021}<B_{MSY}$ and $F_{2021}<F_{MSY}$] = 72.82%)

1. Introduction

Here, we present an updated stock assessment of Pacific saury in the WNPO of the North Pacific Fisheries Commission (NPFC) convention area. The assessment consisted of applying the Bayesian state-space surplus production model with available catches and standardized catch-per-unit-effort (CPUE) indices from the members from 1980 to 2021 and the Japanese biomass index from 2003-2022. The Bayesian method provided direct estimates of the uncertainty of the model parameters and management quantities. The objectives of this study are to conduct a stock assessment for the Pacific saury in the WNPO through 2021, to examine the sensitivity of the results to changes in model structural uncertainty, and to determine the ensemble stock condition from the developed base cases. Since the SSC PS agreed not to conduct the stock projections due to the poor predictive ability of the current Bayesian surplus production model (NPFC-2020-SSC PS06-Final Report), therefore we did not include the stock projection and its risk analysis in this updated stock assessment report.

2. Material and methods

Fishery catch data from 1950 – 2021 for assessing WNPO saury were taken from the most recent summary of available fishery-dependent data (NPFC-2022-SSC PS09-WP01). The commercial catch of Pacific saury caught by Japan, Chinese Taipei, Korea, China, Russia, and other members in the WNPO area were collected from 1950 to 2021 (**Figure 1**). Estimates of standardized fishery-dependent catch-per-unit-effort (CPUE) of WNPO saury were available for Japanese offshore stick-held dip net fisheries, however, Japanese standardized CPUE data were separated into two time-series, one before 1994 (1980 – 1993) (NPFC-TWG PSSA03-WP11) and one from 1994 to 2021 (NPFC-2022-SSC PS09-WP08) to account for the potential change in catchability. Indices of Chinese Taipei and Korean distant-water stick-held dip net fisheries were available from 2001 – 2021 (NPFC-2022-SSC PS09-WP04 and NPFC-2022-SSC PS09-WP09(Rev 2)). Russia provided the abundance index of offshore and distant stick-held dip net fisheries from 1994 – 2021 (NPFC-2022-SSC PS09-WP03). An index of Chinese distant-water stick-held dip net fisheries was also available from 2013 - 2021 (NPFC-2022-SSC PS09-WP06). The joint CPUE index was available from 1994 – 2021 (NPFC-2022-SSC PS09-WP05(Rev 1)). Fishery-independent biomass index was available from Japanese scientific research surveys from 2003 – 2022 (NPFC-2022-SSC PS09-WP07(Rev 1)) (**Figure 2**). Based on the agreed configuration of the base case scenarios by SSC PS09 (NPFC-2022-SSC PS09-Final Report), the specification of the two base case models was shown in **Table 1**. In addition, two sensitivity cases were developed to evaluate the impacts of the inclusion of the early Japanese CPUE with time-varying catchability (**Table 1**). The Bayesian analysis requires prior probability distributions for each of the model parameters. These priors were summarized in **Table 2**.

3. Results

3.1 Convergence of base case model

The visual inspection of trace plots of the major parameters showed the good mixing of the three chains (i.e., moving around the parameter space), also indicative of convergence of the MCMC chains. The Gelman and Rubin statistic for all parameters, including all variance terms, equaled 1, which indicated convergence of the Markov chains. Similarly, the Heidelberger and Welch test could not reject the hypothesis that the MCMC chains were stationary at the 95% confidence level for any of the parameters. Overall, these diagnostics indicated that the posterior distributions of the model parameters were adequately sampled with the MCMC simulations.

3.2 Model fits to catch-per-unit-effort indices

Plots of residual diagnostics by fishery for the base case models were shown in **Figures 3 and 4**. For base case 1, models fit to the Chinese Taipei index had a residual trend with negative residuals in 2002 – 2010 and positive residuals in 2011 – 2020 (**Figure 3**). The base model 2 fits to the joint CPUE and the Japanese survey index did not show a residual pattern over years (**Figure 4**).

3.3 Posterior estimates of model parameters

Plots of posterior densities of the parameters r (intrinsic growth rate), K (carrying capacity), M (shape parameter), σ^2 (observation error), τ^2 (process error), b (Hyper-depletion/stability), and P_1 (biomass depletion in 1980) for each base case were shown in **Figures 5 – 6**. Summaries of parameter estimates of each of the base cases and the sensitivity cases were provided in **Tables S1 – S4**. The results of time-varying catchability (q) in early Japanese CPUE (1980 – 1993) for two sensitivity cases were shown in **Figure S1**.

3.4 Stock assessment results

Time-series of exploitable biomass (B), the ratio of biomass to B_{MSY} (B/B_{MSY}) and the biomass depletion (B/K) of the base case models and sensitivity cases were provided in **Figures 7 and Figures S2 – S5**. Similar trends in biomass were found in the two base cases. The ensemble time-series of biomass is estimated to have an increasing pattern since 2000, with two peaks in 2003 and 2005, after then decreased overtime and below B_{MSY} in 2009 – 2022. It should be noted that the models estimate the lowest biomass level in 2020 (median B_{2020}/B_{MSY} = 0.29, 80 percentile range 0.18 – 0.51) and following a slight increase in 2021 and 2022 (median B_{2021}/B_{MSY} = 0.33, 80 percentile range 0.19 – 0.56; median B_{2022}/B_{MSY} = 0.45, 80 percentile range 0.23 – 0.77) (**Figure 7 and Table 3**). In the recent three years (2020 – 2022), the average biomass was estimated below the B_{MSY} (median $B_{2020\text{-}2022}/B_{MSY}$ = 0.36, 80 percentile range 0.20 – 0.60).

Time-series of the fishing mortality (F) and the ratio of fishing mortality to (F/F_{MSY}) of the base cases and sensitivity cases were shown in **Figure 8 and Figures S6 – S9**. The trend of fishing mortality in base cases 1 and 2 was similar. The ensemble time-series of the fishing mortality ratio trend from two base cases was shown in **Figure 8**. The fishing mortality was below F_{MSY} before 2007, and then the fishing mortality increased above F_{MSY} and reached a high level in 2014 and 2018, respectively. A decreased trend in fishing mortality was found from 2019 to 2021. The recent average fishing mortality is estimated to be above F_{MSY} (median $F_{2019\text{-}2021}/F_{MSY}$ = 1.21, 80 percentile range = 0.71 – 2.16) while the fishing mortality in 2021 is less than F_{MSY} (median F_{2021}/F_{MSY} = 0.75, 80 percentile range = 0.43 – 1.45).

The quantities of management interest reference points from joint estimates of the base case 1 and 2 were shown in **Table 3**, and each of the base cases and the sensitivity cases was shown in **Tables S5 – S8**, respectively. Overall, the ensemble MCMC results from the two base cases indicated that the 2021 stock status is likely within the yellow quadrant (Prob [$B_{2021}<B_{MSY}$ and $F_{2021}<F_{MSY}$] = 72.82%) (**Figure 9**). The stock conditions derived from the ensemble MCMC results of the two base cases for the last year and for the recent three years were also shown in the Kobe plots (**Figure 10)**.

3.5 Retrospective analysis

Time-series of B/B_{MSY} and F/F_{MSY} estimated by each of the base cases with the removal of the most five years of data (catch: 2016 – 2020; Japan biomass survey: 2017 – 2021) in successive model were shown in **Figures 11 – 12**. It suggested that there is generally no consistent pattern of bias in the estimates of B/B_{MSY} and F/F_{MSY} for the base case 1, but a slightly bias for the base case 2.

References

NPFC (2019). Additional information regarding changes in the Japanese stick-held dip net for Pacific saury, especially in 1980s. NPFC-TWG PSSA03-WP11

NPFC (2020). Small Scientific Committee on Pacific Saury. 2020. 6th Meeting Report. NPFC-2020-SSC PS06-Final Report. 68 pp. (Available at www.npfc.int)

NPFC (2022). Small Scientific Committee on Pacific Saury. 2022. 9th Meeting Report. NPFC-2022-SSC PS09-Final Report. 23 pp. (Available at www.npfc.int)

NPFC (2022). Compiled data on Pacific saury catches in the northwestern Pacific Ocean. NPFC-2022-SSC PS09-WP01.

NPFC (2022). CPUE standardization for the Pacific saury Russian catches in the Northwest Pacific Ocean. NPFC-2022-SSC PS09-WP03

NPFC (2022). Standardized CPUE of Pacific saury (*Cololabis saira*) caught by the Chinese Taipei stick-held dip net fishery up to 2021. NPFC-2022-SSC PS09-WP04

NPFC (2022). Joint CPUE standardization of the Pacific saury in the Northwest Pacific Ocean by using the spatio-temporal modelling approach. NPFC-2022-SSC PS09-WP05(Rev 1)

NPFC (2022). Standardized CPUE of Pacific saury (*Cololabis saira*) caught by the China's stick-held dip net fishery up to 2021. NPFC-2022-SSC PS09-WP06

NPFC (2022). Japanese survey biomass index of Pacific saury up to 2022 using VAST model. NPFC-2022-SSC PS09-WP07(Rev.1)

NPFC (2022). Standardized CPUE of Pacific saury (*Cololabis saira*) caught by the Japanese stick-held dip net fishery up to 2021. NPFC-2022-SSC PS09-WP08

NPFC (2022). Standardized CPUE of Pacific saury (*Cololabis saira*) caught by the Korean's stick-held dip net fishery up to 2021. NPFC-2022-SSC PS09-WP09(Rev 2)

Table 1. Specifications of the two base case models and four sensitivity case models. “JPN_early” = early Japan (1980 – 1993), “JPN_late” = late Japan (1994 – 2021), “CT” = Chinese Taipei, “RUS” = Russia, “KOR” = Korea, “CHN” = China, “JPN_bio” = Japan biomass survey (NPFC-2022-SSC PS09-Final Report).

<table>
<tr><th>Model</th><th>Base case 1 (NB1)</th><th>Base case2 (NB2)</th><th>Sensitivity case1 (NS1)</th><th>Sensitivity case2 (NS2)</th></tr>
<tr><td>Initial year</td><td colspan="4">1980</td></tr>
<tr><td>Biomass survey</td><td colspan="4">$I_{bio,t} = q_{bio} B_t e^{v_{bio,t}}$
$V_{bio,t} \sim N(0, cv_{bio,t}^2 + \sigma^2)$
$q_{bio} \sim U(0,1)(2003-2022)$</td></tr>
<tr><td>Fleet CPUEs and Joint CPUE</td><td>CHN (2013 – 2021)
JPN_late (1994–2021)
KOR (2001 – 2021)
RUS (1994 – 2021)
CT (2001 – 2021)
$I_{f,t} = q_f B_t^b e^{v_{f,t}}$
$v_{f,t} \sim N(0, \sigma_f^2)$
$\sigma_f^2 = c \bullet (ave(cv_{bio,t}^2) + \sigma^2)$
where $ave(cv_{bio,t}^2)$ is computed except for the 2020 biomass survey (*c*=5)</td><td>Joint CPUE (1994-2021)
$I_{joint,t} = q_{joint} B_t^b e^{v_{joint,t}}$
$v_{joint,t} \sim N(0, cv_{joint,t}^2 + \sigma^2)$</td><td>CHN (2013 – 2021)
JPN_early (1980 – 1993, time-varying *q*)
JPN_late (1994–2021)
KOR (2001 – 2021)
RUS (1994 – 2021)
CT (2001 – 2021)
$I_{f,t} = q_f B_t^b e^{v_{f,t}}$
$v_{f,t} \sim N(0, \sigma_f^2)$
$\sigma_f^2 = c \bullet (ave(cv_{bio,t}^2) + \sigma^2)$
where $ave(cv_{bio,t}^2)$ is computed except for the 2020 biomass survey (*c*=6)</td><td>JPN_early (1980 – 1993, time-varying *q*)
$I_{JE,t} = q_{JE} B_t^b e^{v_{JE,t}}$
$v_{JE,t} \sim N(0, \sigma_{JE}^2)$
$\sigma_{JE}^2 = c \bullet (ave(cv_{joint,t}^2) + \sigma^2)$

Joint CPUE (1994 – 2021)
$I_{joint,t} = q_{joint} B_t^b e^{v_{joint,t}}$
$v_{joint,t} \sim N(0, cv_{joint,t}^2 + \sigma^2)$</td></tr>
<tr><td>Hyper-depletion/ stability</td><td colspan="2">A common parameter for all fisheries with a prior distribution, *b* ~ U(0, 1)</td><td>A common parameter for all fisheries but JPN_early, with a prior distribution, *b* ~ U(0, 1)
[b for JPN_early is fixed at 1]</td><td>*b* ~ U (0, 1) for joint CPUE.
[b for JPN_early is fixed at 1]</td></tr>
<tr><td>Prior for other than q_{bio}</td><td colspan="4">Own preferred options</td></tr>
</table>

Table 2. Summary of the specified priors for the Bayesian state-space models. "JPN1" = early Japan (1980 – 1993), "JPN2" = late Japan (1994 – 2021), "CT" = Chinese Taipei, "RUS" = Russia, "KOR" = Korea, "CHN" = China, "JPN_bio" = Japan biomass survey.

Parameter	**Description**	**Prior**
K	Carrying capacity (10,000 mt)	$K \sim U(60,1900)$
r	Intrinsic growth rate (year^{-1})	$r \sim U(0,3)$
M	Shape parameter	$M \sim U(0,3)$
q	Catchability for fleets (JPN2; CT; RUS; KOR; CHN and Joint CPUE)	$1/q \sim Gamma(0.01,0.01)$
q_{bio}	catchability for Japanese survey biomass	$q_{bio} \sim U(0,1)$
q_{JPN1}^{1980}	Time-varying catchability for JPN1 in 1980	$q_{JPN1}^{1980} \sim U(1\times10^{-1},1)$
ω	Annual deviation of log-scale time-varying catchability	$\omega \sim N(0,0.1)$
β	Hyperstability of 1994 - 2021	$\beta \sim U(0,1)$
σ^2	Common observation error of CPUE	$1/\sigma^2 \sim Gamma(2,0.45)$
τ^2	Process error	$1/\tau^2 \sim Gamma(4,0.1)$
P_1	Initial condition (B_1/K)	$P_1 \sim U(0,1)$

Table 3. Summary of joint estimates of reference points of the base cases 1 and 2.

	Mean	Median	Lower 10th	Upper 10th
$Catch_{2021}$	9.22	9.22	9.22	9.22
$F_{2019\text{-}2021}$	0.28	0.24	0.08	0.55
F_{2021}	0.17	0.15	0.05	0.33
F_{MSY}	0.24	0.21	0.06	0.46
MSY	39.26	38.85	26.61	49.79
F_{2021}/F_{MSY}	1.22	0.75	0.43	1.45
$F_{2019\text{-}2021}/F_{MSY}$	1.86	1.21	0.71	2.16
K	565.04	398.25	177.80	1274.00
B_{2021}	90.51	61.96	28.19	176.10
B_{2022}	114.45	82.04	42.16	212.07
$B_{2020\text{-}2022}$	96.89	66.88	32.23	185.61
B_{MSY}	261.02	186.40	90.58	563.27
B_{MSY}/K	0.62	0.47	0.20	1.12
B_{2021}/K	0.17	0.16	0.08	0.27
B_{2022}/K	0.23	0.22	0.10	0.37
$B_{2020\text{-}2022}/K$	0.19	0.18	0.09	0.29
B_{2021}/B_{MSY}	0.36	0.33	0.19	0.56
B_{2022}/B_{MSY}	0.49	0.45	0.23	0.77
$B_{2020\text{-}2022}/B_{MSY}$	0.39	0.36	0.20	0.60

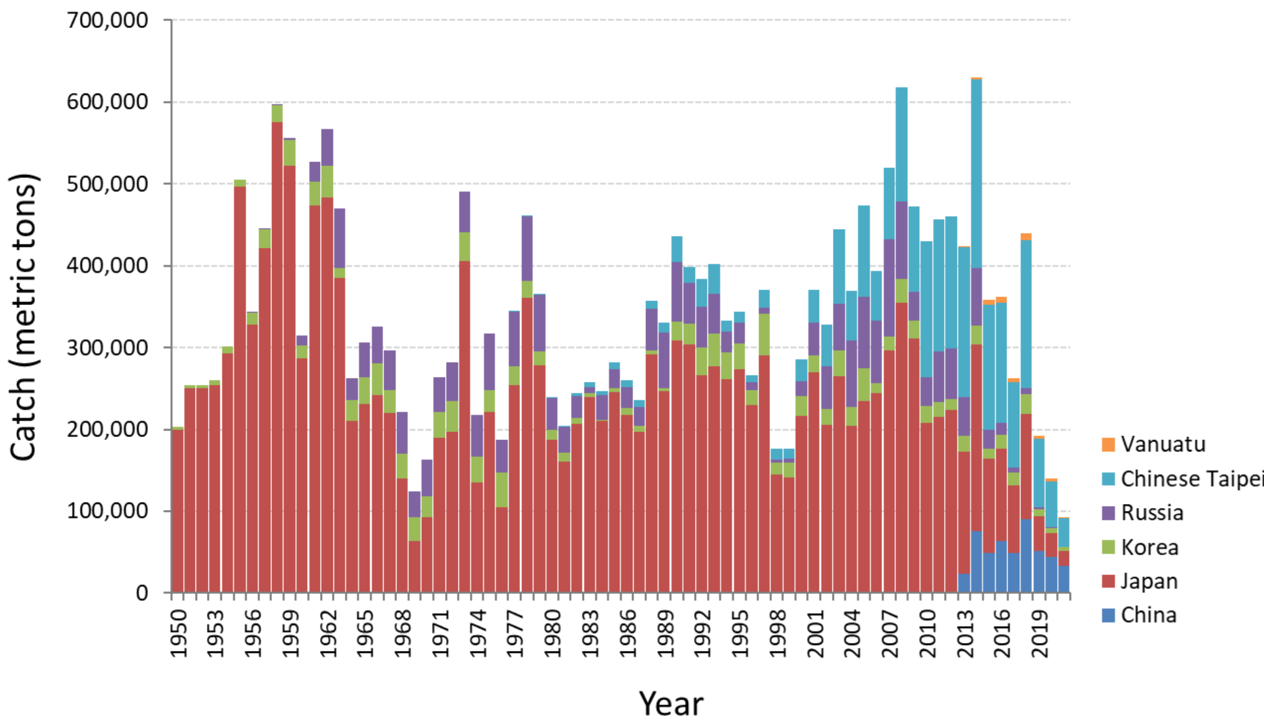

Figure 1. Time-series of catches (in metric ton) of the Pacific saury in the Western North Pacific Ocean from 1950 to 2021 by the members.

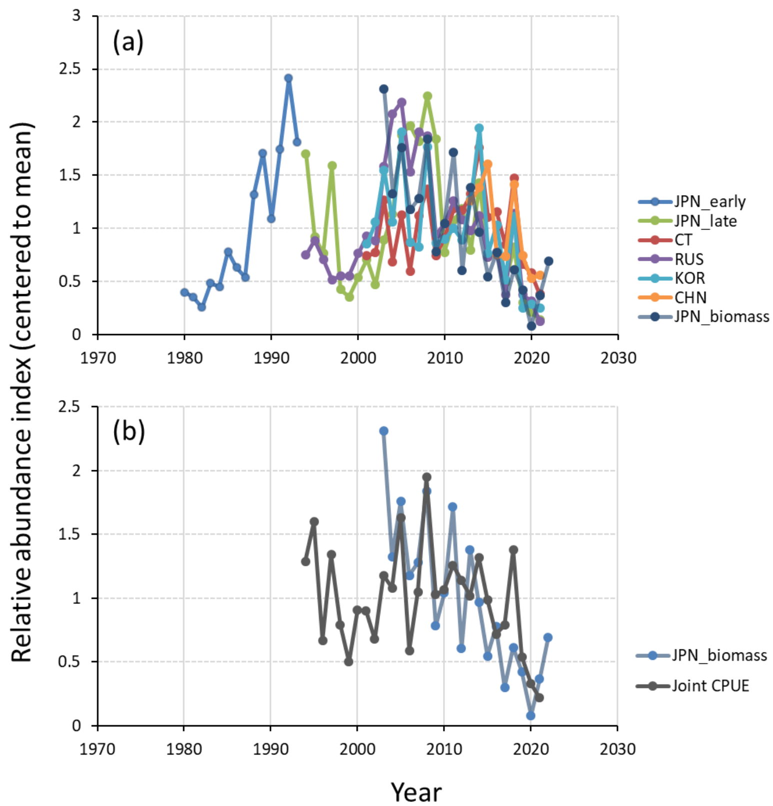

Figure 2. (a) Pacific saury CPUE indices from early Japan (JPN_early), late Japan (JPN_late), Chinese Taipei (CT), Russia (RUS), Korea (KOR), and China (CHN) stick-held dip net fisheries, and biomass survey index of Japan (JPN_biomass) during 1980 – 2022 and (b) time-series of biomass survey index of Japan (JPN_biomass) and joint CPUE during 1994 – 2021 in the Western North Pacific Ocean.

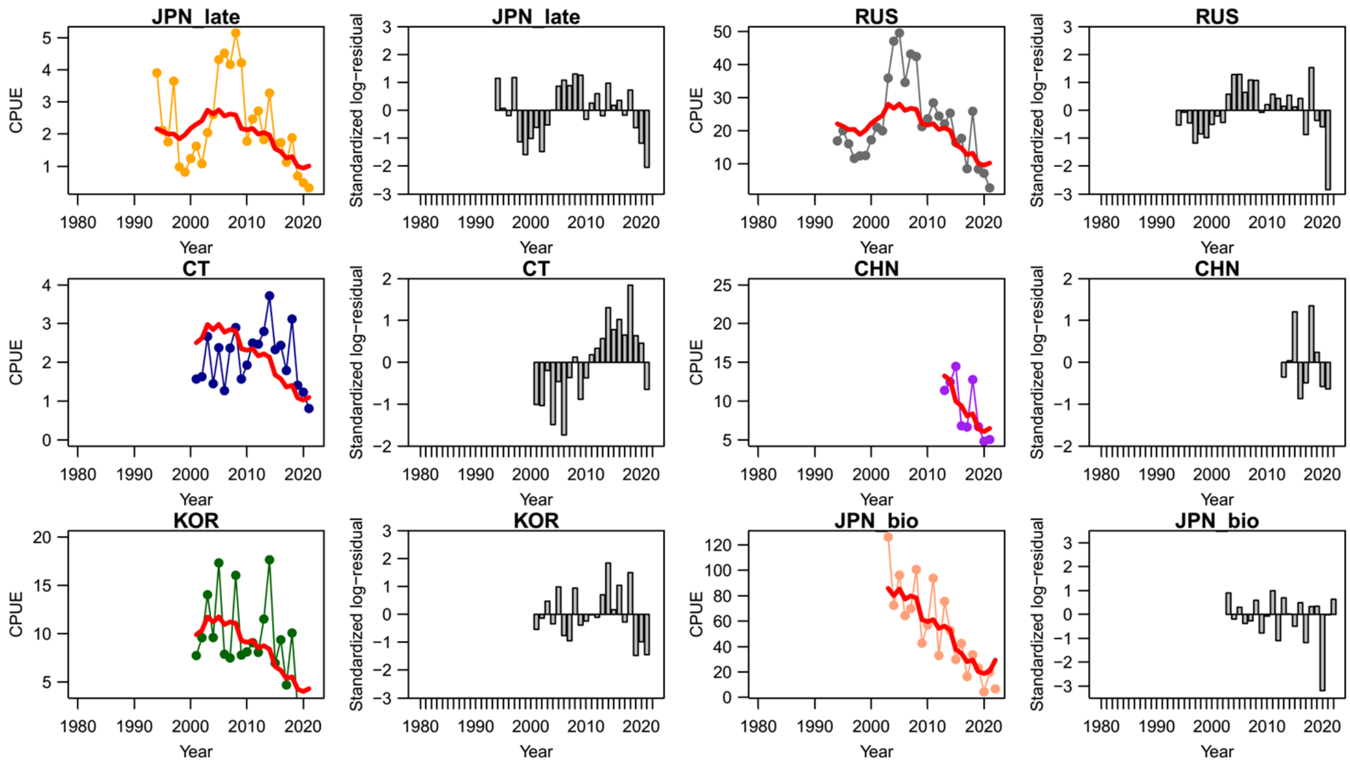

Figure 3. Time-series of observed (circle-line) and predicted (red solid line) catch per unit effort (CPUE) of Western North Pacific saury and standardized log-residuals for the base case 1 production model. “JPN_early” = early Japan (1980-1993), “JPN_late” = late Japan (1994-2021), “CT” = Chinese Taipei, “RUS” = Russia, “KOR” = Korea, “CHN” = China, JPN_bio” = Japanese biomass survey.

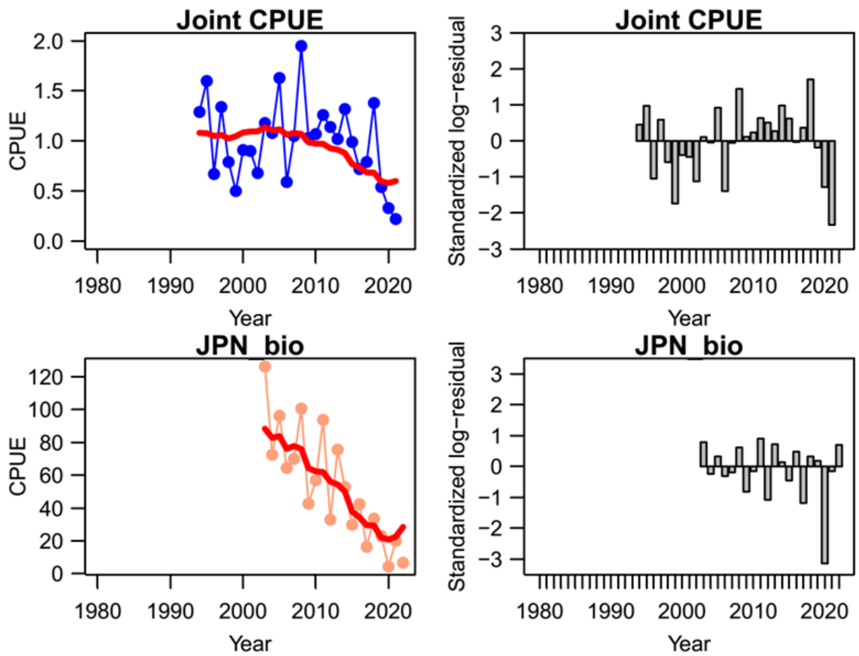

Figure 4. Time-series of observed (circle-line) and predicted (red solid line) catch per unit effort (CPUE) of Western North Pacific saury and standardized log-residuals for the base case 2 production model. "Joint CPUE" = joint CPUE index (1994 – 2021), and "JPN_bio" = Japanese biomass survey.

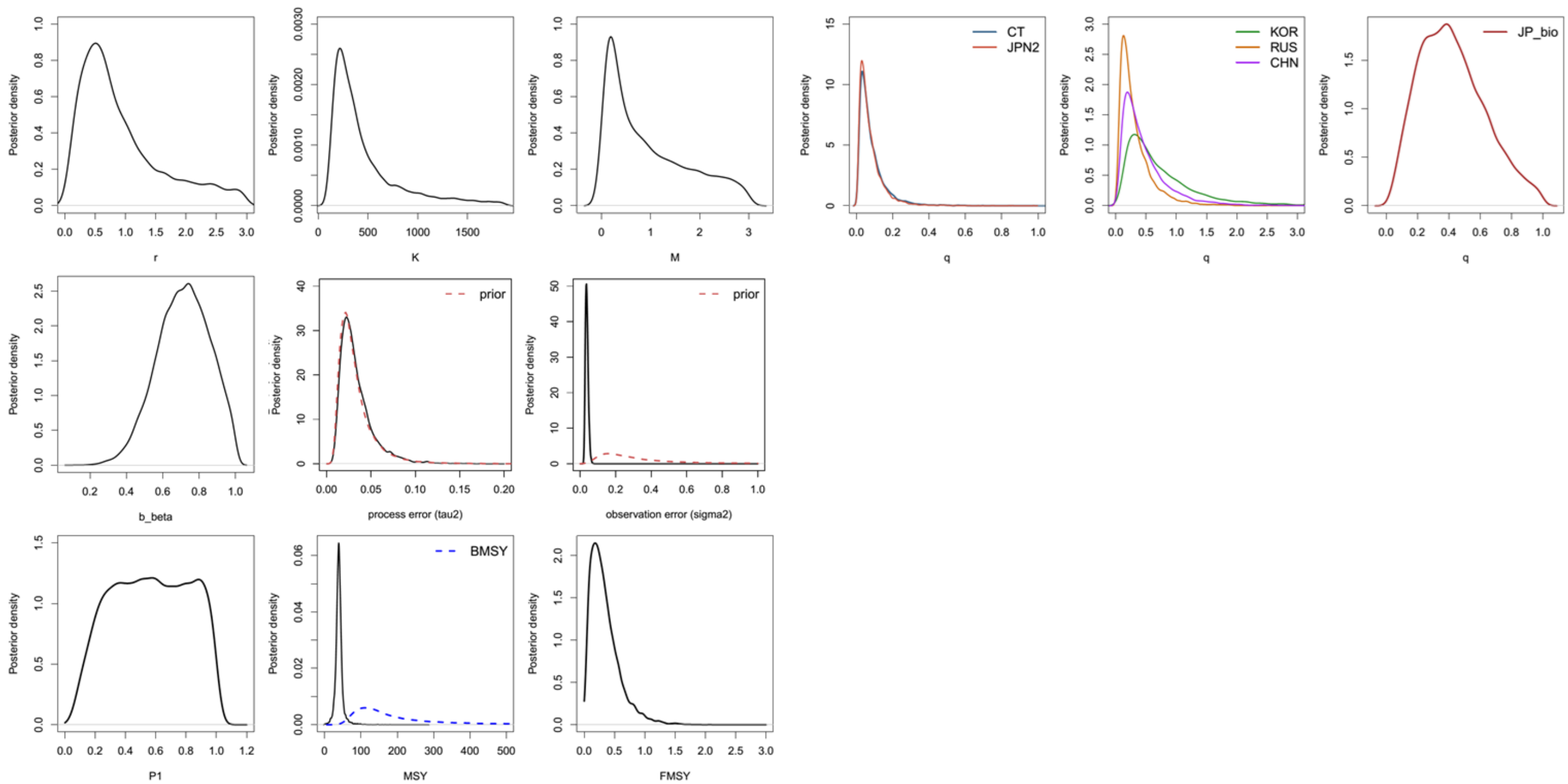

Figure 5. Kernel density estimates of the posterior distributions (solid lines) of various model parameters and management quantities for the base case 1 production model for the Pacific saury in the Western North Pacific Ocean. Proper prior densities are given by the dashed lines. “JPN2” = late Japan (1994-2021), “CT” = Chinese Taipei, “RUS” = Russia, “KOR” = Korea, “CHN” = China, “JP_bio” = Japanese biomass survey.

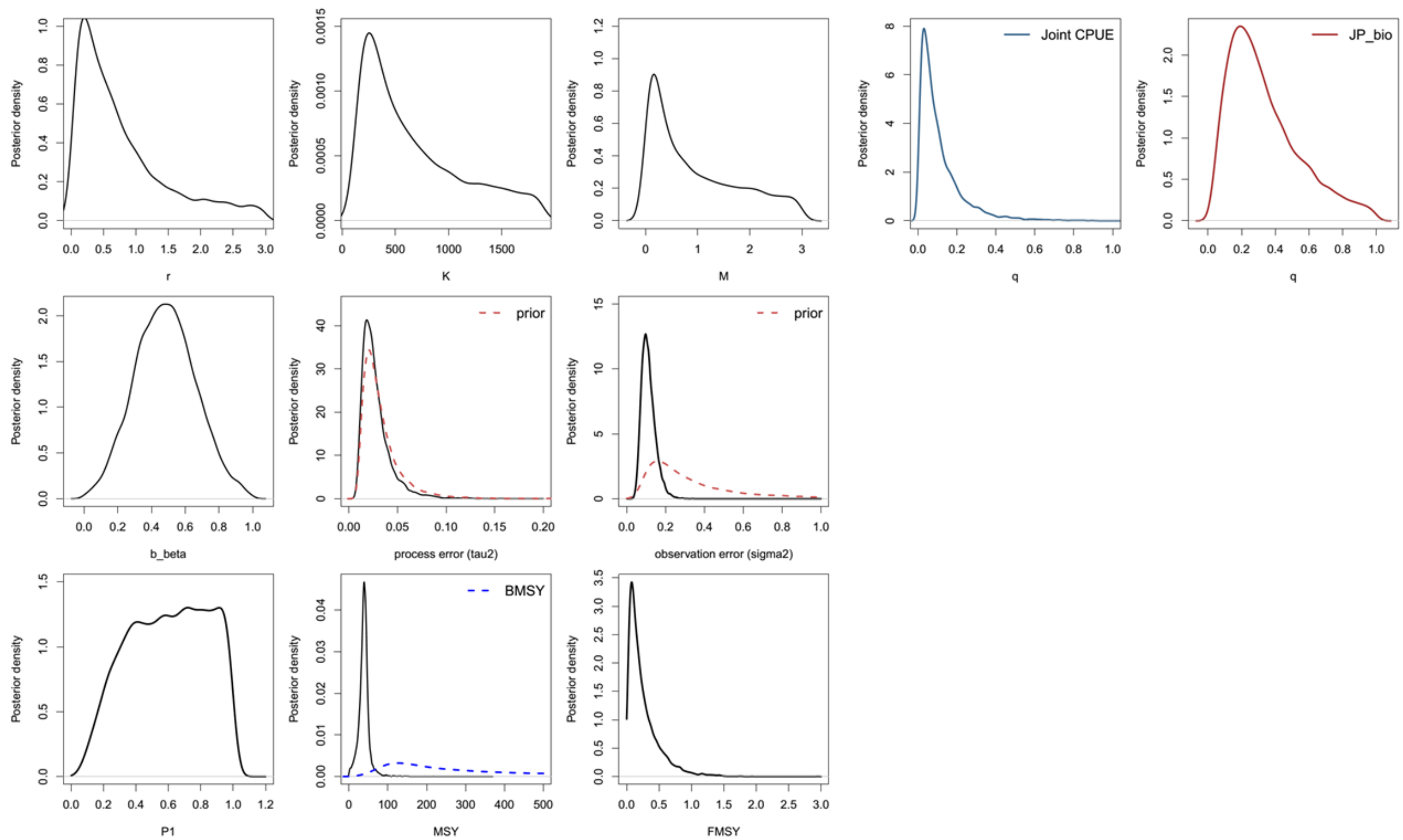

Figure 6. Kernel density estimates of the posterior distributions (solid lines) of various model parameters and management quantities for the base case 2 production model for the Pacific saury in the Western North Pacific Ocean. Proper prior densities are given by the dashed lines. “Joint CPUE” = Joint CPUE index, “JP_bio” = Japanese biomass survey.

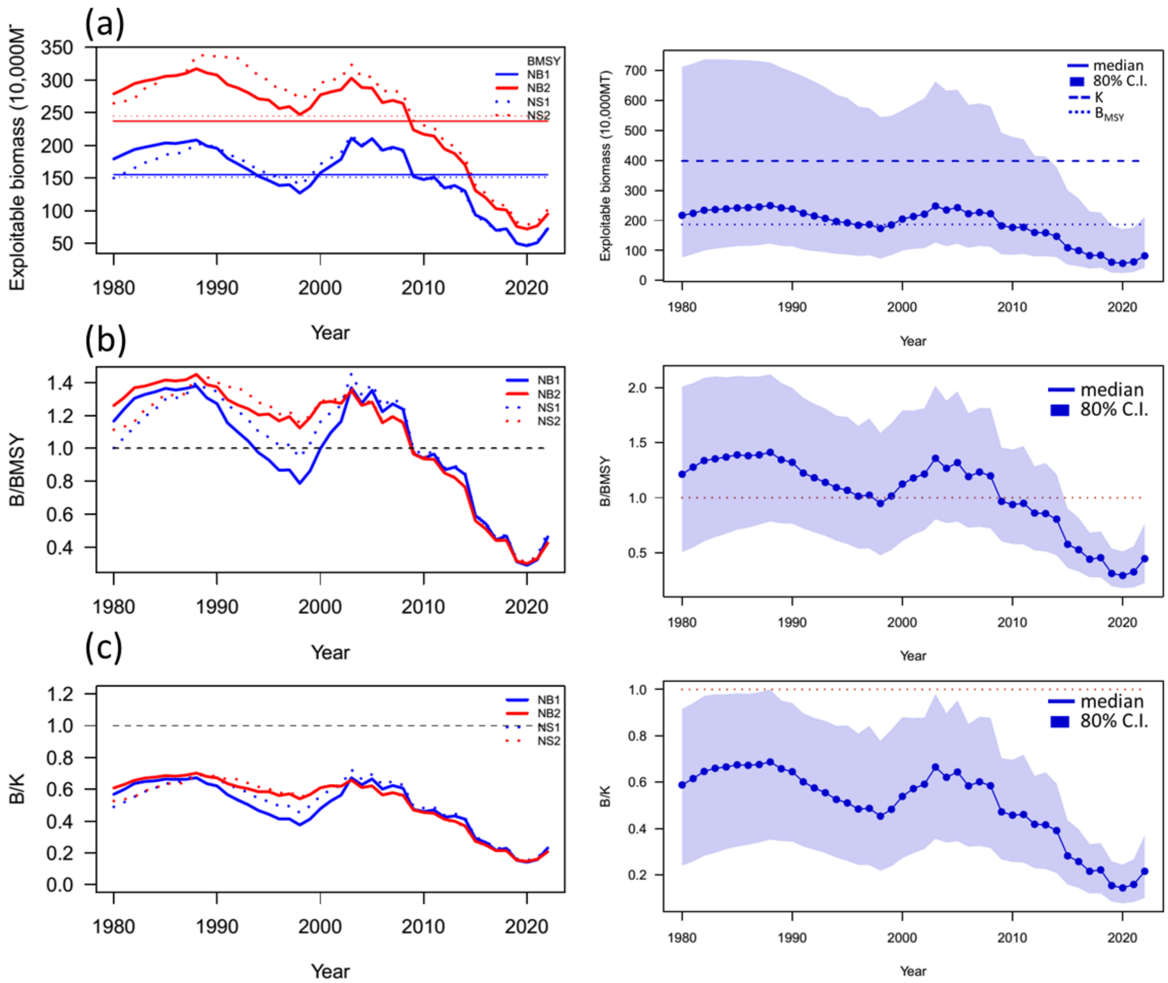

Figure 7. Time series of ensemble biomass (10,000 metric ton) (a), the ratio of biomass to B_{MSY} (B/B_{MSY}) (b), and the depletion ratio (B/K) (c) of the western North Pacific saury for the base case 1 – 2 (NB1 and NB2) and sensitivity case (NS1 and NS2, respectively; left panel) and the median estimates of MCMC results from base cases 1 – 2 (right panel). In panel (a), the dashed horizontal line denotes the B_{MSY}. In panels (b) and (c), the dashed lines denote the reference levels of 1.

(a)

(b)

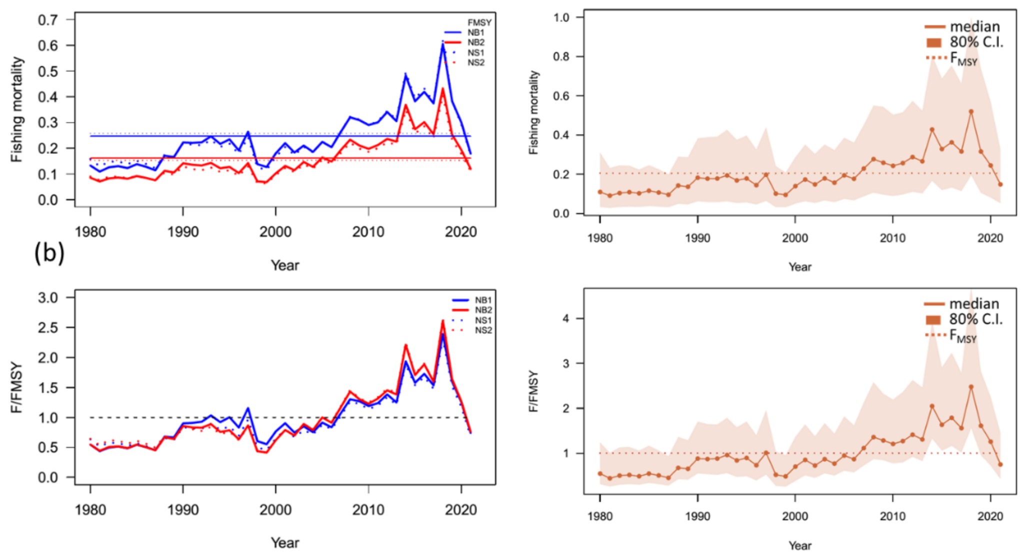

Figure 8. Time series of fishing mortality (a) and the ratio of biomass to F_{MSY} (F/F_{MSY}) (b) of the western North Pacific saury for the base case 1 – 2 (NB1 and NB2) and sensitivity case (NS1 and NS2, respectively; left panel) and the median estimates of MCMC results from base cases 1 – 2 (right panel). In panel (a), the dashed horizontal line denotes the F_{MSY}. In panels (b), the dashed lines denote the reference levels of 1.

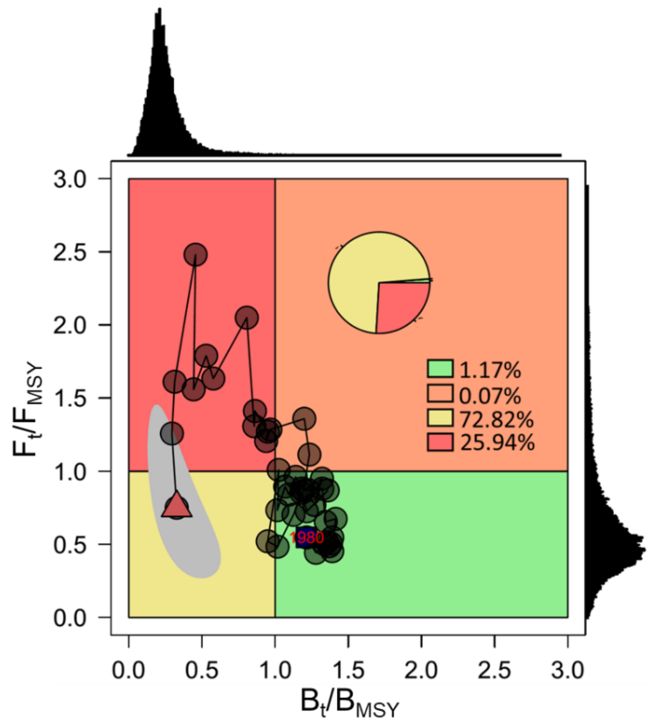

Figure 9. Ensemble Kobe phase plot of the stock trajectory of the western North Pacific saury from 1980 to 2021 (in a red triangle) with uncertainty estimate in 2021 (80% credible intervals, grey polygon) from the two base case models.

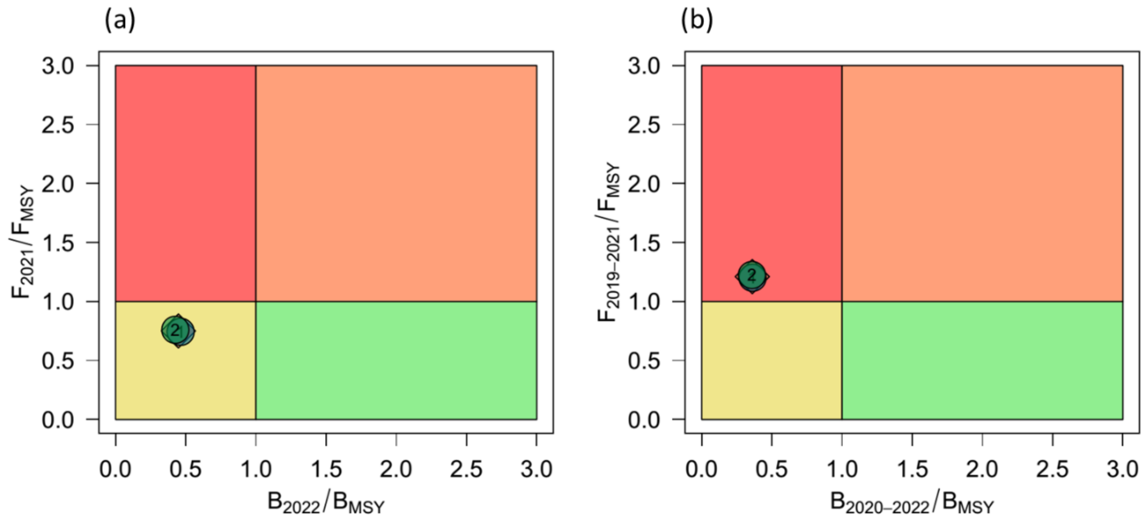

Figure 10. Kobe phase plot of stock status in the (a) last year and (b) recent three years (B2020 – 2022 and F2019 – 2021) of Pacific saury from the two base case models. The orange diamond is the median estimate of MCMC results from the two base case models.

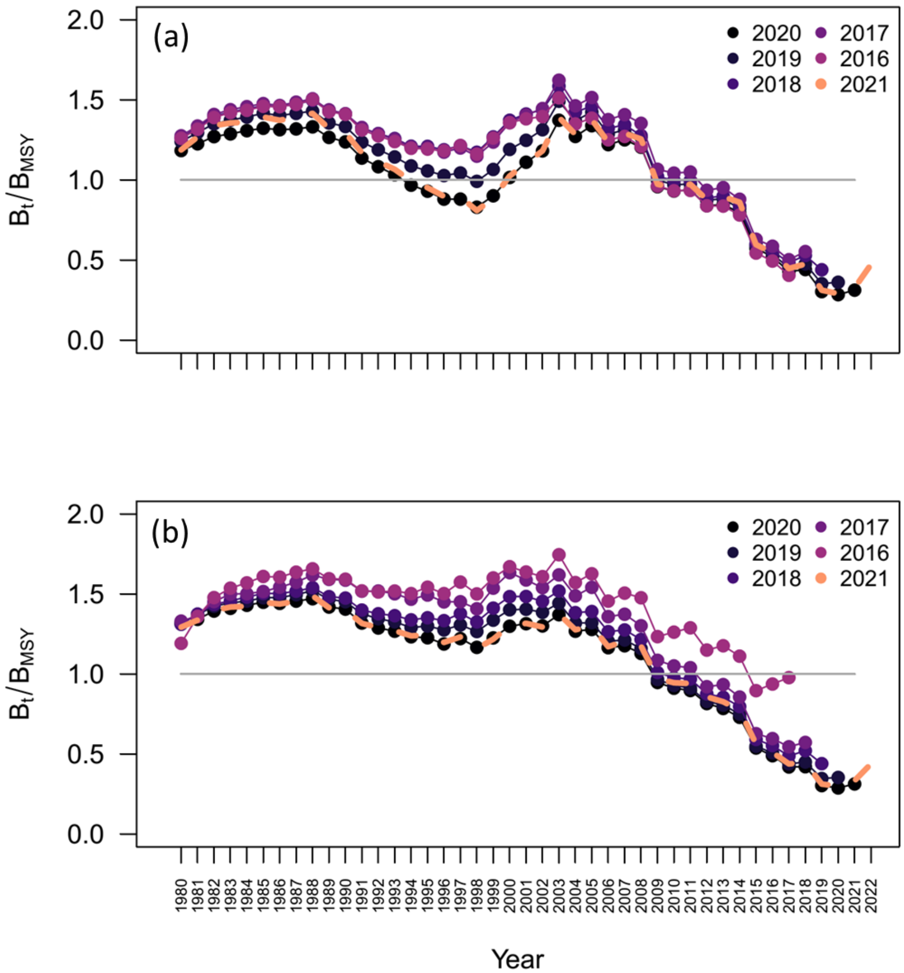

Figure 11. Five years within-model retrospective plots of the change in biomass to B_{MSY} of the western North Pacific saury from the base case 1 (a) and 2 (b).

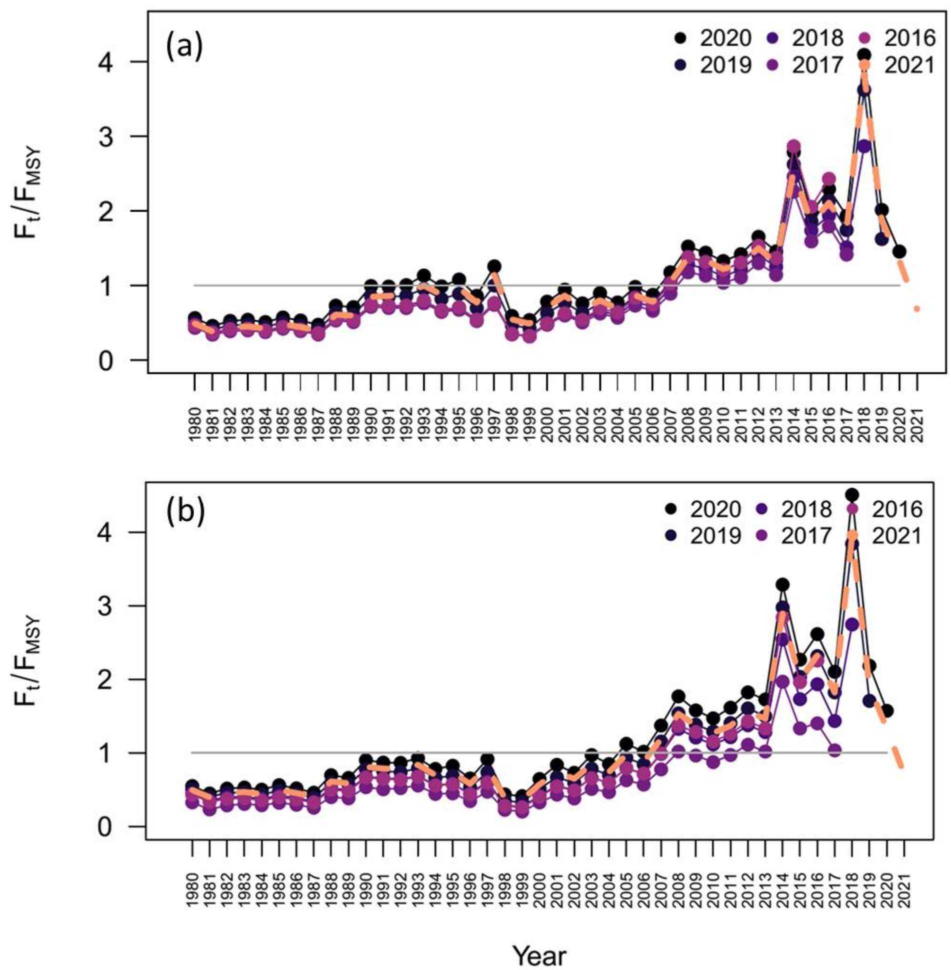

Figure 12. Five years within-model retrospective plots of the change in fishing mortality to F_{MSY} of the western North Pacific saury from the base case 1 (a) and 2 (b).

Table S1. Summary of parameter estimates of the base case 1.

	Mean	Median	Lower 10th	Upper 10th
r	0.93	0.71	0.24	2.05
K	461.13	334.05	168.60	979.08
qJPN2	0.08	0.06	0.13	0.99
qCT	0.08	0.06	0.02	0.17
qKOR	0.33	0.24	0.09	0.68
qRUS	0.79	0.57	0.21	1.58
qCHN	0.49	0.36	0.13	0.99
qBio	0.42	0.40	0.17	0.72
Shape parameter (*M*)	0.95	0.69	0.11	2.30
observation error (σ_{com})	0.19	0.19	0.17	0.22
observation error (σ_{bio})	0.09	0.09	0.07	0.10
process error (τ)	0.18	0.17	0.13	0.24
F_{MSY}	0.27	0.25	0.09	0.48
B_{MSY}	212.03	155.50	86.45	425.58
MSY	39.83	39.03	29.72	48.79
b	0.71	0.72	0.52	0.90

Table S2. Summary of parameter estimates of the base case 2.

	Mean	Median	Lower 10th	Upper 10th
r	0.78	0.55	0.12	1.89
K	668.95	513.95	192.71	1447.90
qBio	0.34	0.28	0.11	0.65
qJoint	0.11	0.07	0.08	2.34
Shape parameter (*M*)	0.96	0.68	0.02	0.25
observation error (σ)	0.33	0.33	0.27	0.40
process error (τ)	0.16	0.15	0.12	0.21
F_{MSY}	0.21	0.16	0.05	0.44
B_{MSY}	310.02	237.25	97.47	645.28
MSY	38.69	38.56	23.23	50.81
b	0.48	0.48	0.25	0.72

Table S3. Summary of parameter estimates of the sensitivity case 1.

	Mean	Median	Lower 10th	Upper 10th
r	0.89	0.70	0.25	1.91
K	430.08	314.05	164.30	870.95
qJPN2	0.02	0.02	0.01	0.04
qCT	0.11	0.08	0.03	0.23
qKOR	0.43	0.30	0.10	0.89
qRUS	1.00	0.70	0.24	2.09
qCHN	0.61	0.44	0.15	1.26
qBio	0.43	0.40	0.17	0.73
Shape parameter (*M*)	1.04	0.80	0.13	2.39
observation error (σ_{com})	0.18	0.18	0.16	0.21
observation error (σ_{bio})	0.08	0.07	0.07	0.09
process error (τ)	0.17	0.16	0.12	0.22
F_{MSY}	0.36	0.30	0.10	0.69
B_{MSY}	201.65	151.25	84.19	391.69
MSY	40.08	39.53	30.56	48.96
b	0.67	0.67	0.46	0.87
q_JPN11980	0.0061	0.0045	0.0015	0.0124
q_JPN11981	0.0058	0.0045	0.0015	0.0117
q_JPN11982	0.0057	0.0045	0.0016	0.0112
q_JPN11983	0.0062	0.0050	0.0018	0.0119
q_JPN11984	0.0067	0.0054	0.0020	0.0128
q_JPN11985	0.0074	0.0062	0.0022	0.0140
q_JPN11986	0.0080	0.0068	0.0025	0.0150
q_JPN11987	0.0090	0.0077	0.0028	0.0168
q_JPN11988	0.0109	0.0093	0.0035	0.0200
q_JPN11989	0.0126	0.0108	0.0040	0.0235
q_JPN11990	0.0139	0.0119	0.0043	0.0261
q_JPN11991	0.0160	0.0136	0.0049	0.0299
q_JPN11992	0.0180	0.0150	0.0053	0.0342
q_JPN11993	0.0189	0.0154	0.0053	0.0363

Table S4. Summary of parameter estimates of the sensitivity case 2.

	Mean	Median	Lower 10th	Upper 10th
r	0.78	0.53	0.12	1.91
K	678.77	538.45	216.10	1411.00
qBio	0.31	0.27	0.10	0.59
qJoint	0.11	0.07	0.08	2.32
Shape parameter (*M*)	0.92	0.60	0.02	0.25
observation error (σ)	0.31	0.31	0.26	0.37
process error (τ)	0.16	0.15	0.12	0.21
F_{MSY}	0.19	0.15	0.05	0.39
B_{MSY}	312.69	244.95	107.20	626.99
MSY	37.75	37.89	22.83	49.78
b	0.48	0.47	0.24	0.71
q_JPN11980	0.0037	0.0025	0.0008	0.0080
q_JPN11981	0.0035	0.0024	0.0008	0.0074
q_JPN11982	0.0033	0.0024	0.0008	0.0068
q_JPN11983	0.0037	0.0028	0.0010	0.0076
q_JPN11984	0.0041	0.0031	0.0011	0.0082
q_JPN11985	0.0048	0.0037	0.0013	0.0095
q_JPN11986	0.0050	0.0039	0.0014	0.0099
q_JPN11987	0.0055	0.0044	0.0016	0.0110
q_JPN11988	0.0072	0.0058	0.0021	0.0143
q_JPN11989	0.0087	0.0070	0.0025	0.0173
q_JPN11990	0.0092	0.0073	0.0026	0.0183
q_JPN11991	0.0110	0.0087	0.0031	0.0223
q_JPN11992	0.0127	0.0101	0.0034	0.0257
q_JPN11993	0.0129	0.0100	0.0034	0.0264

Table S5. Summary of reference points of the base case 1.

	Mean	Median	Lower 10th	Upper 10th
$Catch_{2021}$	9.22	9.22	9.22	9.22
$F_{2019\text{-}2021}$	0.32	0.29	0.11	0.57
F_{2021}	0.20	0.18	0.07	0.35
F_{MSY}	0.27	0.25	0.09	0.48
MSY	39.83	39.03	29.72	48.79
F_{2021}/F_{MSY}	0.87	0.74	0.47	1.25
$F_{2019\text{-}2021}/F_{MSY}$	1.37	1.20	0.78	1.90
K	461.13	334.05	168.60	979.08
B_{2021}	69.86	51.39	26.69	126.30
B_{2022}	95.83	72.59	40.91	165.99
$B_{2020\text{-}2022}$	76.86	57.03	30.93	137.56
B_{MSY}	212.03	155.50	86.45	425.58
B_{MSY}/K	0.48	0.47	0.39	0.59
B_{2021}/K	0.17	0.16	0.09	0.25
B_{2022}/K	0.24	0.23	0.12	0.37
$B_{2020\text{-}2022}/K$	0.18	0.18	0.10	0.28
B_{2021}/B_{MSY}	0.35	0.32	0.20	0.51
B_{2022}/B_{MSY}	0.50	0.46	0.26	0.75
$B_{2020\text{-}2022}/B_{MSY}$	0.39	0.36	0.22	0.56

Table S6. Summary of reference points of the base case 2.

	Mean	Median	Lower 10th	Upper 10th
$Catch_{2021}$	9.22	9.22	9.22	9.22
$F_{2019\text{-}2021}$	0.24	0.19	0.06	0.51
F_{2021}	0.15	0.12	0.04	0.30
F_{MSY}	0.21	0.16	0.05	0.44
MSY	38.69	38.56	23.23	50.81
F_{2021}/F_{MSY}	1.57	0.76	0.39	1.68
$F_{2019\text{-}2021}/F_{MSY}$	2.35	1.22	0.66	2.47
K	668.95	513.95	192.71	1447.90
B_{2021}	111.16	77.03	30.72	219.30
B_{2022}	133.06	95.12	43.84	252.99
$B_{2020\text{-}2022}$	116.93	81.91	34.34	228.55
B_{MSY}	310.02	237.25	97.47	645.28
B_{MSY}/K	0.48	0.47	0.38	0.60
B_{2021}/K	0.18	0.16	0.08	0.29
B_{2022}/K	0.23	0.21	0.09	0.38
$B_{2020\text{-}2022}/K$	0.19	0.17	0.08	0.31
B_{2021}/B_{MSY}	0.37	0.33	0.18	0.61
B_{2022}/B_{MSY}	0.48	0.43	0.21	0.80
$B_{2020\text{-}2022}/B_{MSY}$	0.40	0.36	0.19	0.65

Table S7. Summary of reference points of the sensitivity case 1.

	Mean	Median	Lower 10th	Upper 10th
$Catch_{2021}$	9.22	9.22	9.22	9.22
$F_{2019\text{-}2021}$	0.32	0.28	0.11	0.57
F_{2021}	0.19	0.17	0.07	0.34
F_{MSY}	0.28	0.26	0.10	0.50
MSY	40.08	39.53	30.56	48.96
F_{2021}/F_{MSY}	1.40	0.69	0.44	1.11
$F_{2019\text{-}2021}/F_{MSY}$	2.02	1.13	0.75	1.72
K	430.08	314.05	164.30	870.95
B_{2021}	73.21	53.32	26.95	133.09
B_{2022}	98.42	73.84	41.22	170.76
$B_{2020\text{-}2022}$	79.67	58.57	31.06	142.03
B_{MSY}	201.65	151.25	84.19	391.69
B_{MSY}/K	0.49	0.48	0.39	0.60
B_{2021}/K	0.18	0.17	0.10	0.26
B_{2022}/K	0.25	0.24	0.13	0.37
$B_{2020\text{-}2022}/K$	0.20	0.19	0.11	0.29
B_{2021}/B_{MSY}	0.37	0.35	0.23	0.53
B_{2022}/B_{MSY}	0.52	0.49	0.30	0.76
$B_{2020\text{-}2022}/B_{MSY}$	0.41	0.39	0.25	0.58

Table S8. Summary of reference points of the sensitivity case 2.

	Mean	Median	Lower 10th	Upper 10th
$Catch_{2021}$	9.22	9.22	9.22	9.22
$F_{2019-2021}$	0.22	0.17	0.06	0.45
F_{2021}	0.14	0.11	0.04	0.27
F_{MSY}	0.19	0.15	0.05	0.39
MSY	37.75	37.89	22.83	49.78
F_{2021}/F_{MSY}	1.13	0.75	0.39	1.61
$F_{2019-2021}/F_{MSY}$	1.72	1.21	0.66	2.37
K	678.77	538.45	216.10	1411.00
B_{2021}	114.68	83.36	34.79	227.70
B_{2022}	137.84	101.80	48.10	260.75
$B_{2020-2022}$	120.67	88.35	38.36	237.42
B_{MSY}	312.69	244.95	107.20	626.99
B_{MSY}/K	0.47	0.46	0.38	0.60
B_{2021}/K	0.18	0.16	0.09	0.29
B_{2022}/K	0.23	0.21	0.10	0.37
$B_{2020-2022}/K$	0.19	0.17	0.09	0.30
B_{2021}/B_{MSY}	0.38	0.34	0.19	0.61
B_{2022}/B_{MSY}	0.48	0.43	0.22	0.77
$B_{2020-2022}/B_{MSY}$	0.41	0.37	0.20	0.64

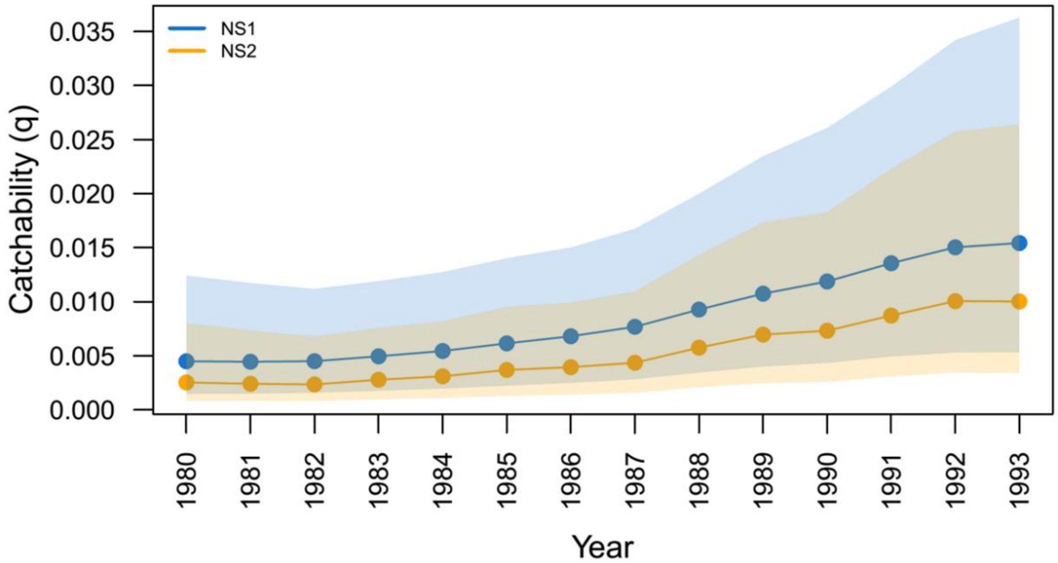

Figure S1. Time series estimates of annual catchabilities of the early Japanese CPUE from 1980 to 1993 for the sensitivity case 1 (NS1) and 2 (NS2).

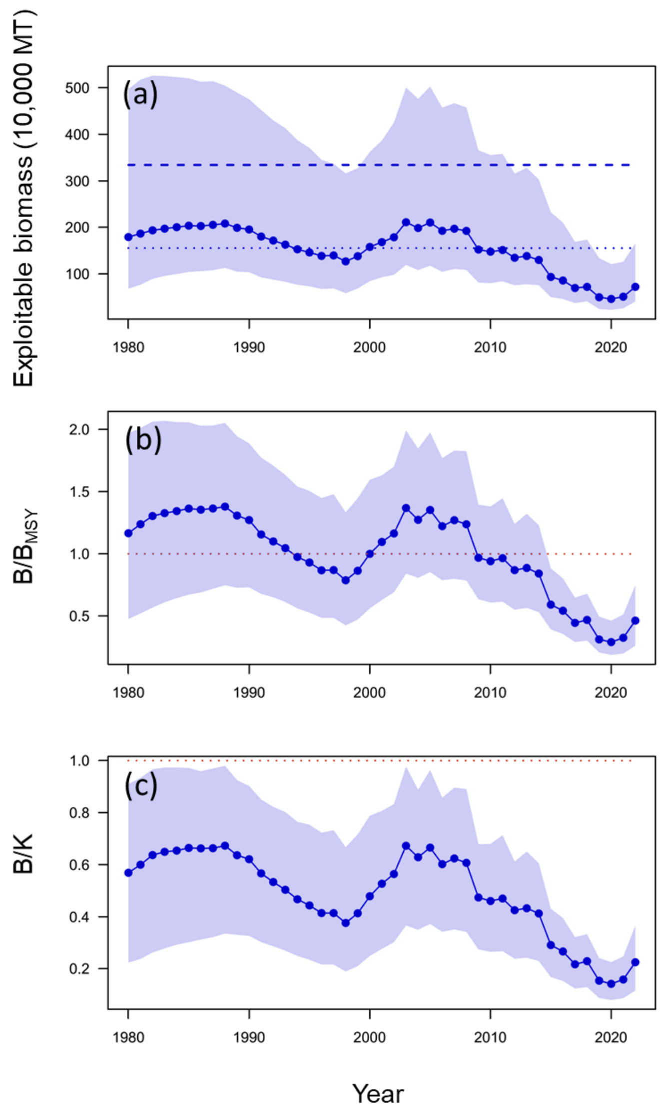

Figure S2. Time series of biomass (10,000 metric tons) (a), the ratio of biomass to B_{MSY} (B/B_{MSY}) (b), and depletion ratio (B/K) (c) of the western North Pacific saury for the base case 1. In panel (a), the upper dashed and lower dotted horizontal line denotes the carrying capacity (K) and B_{MSY}, respectively. In panels (b) and (c), the dashed lines denote the reference levels of 1.

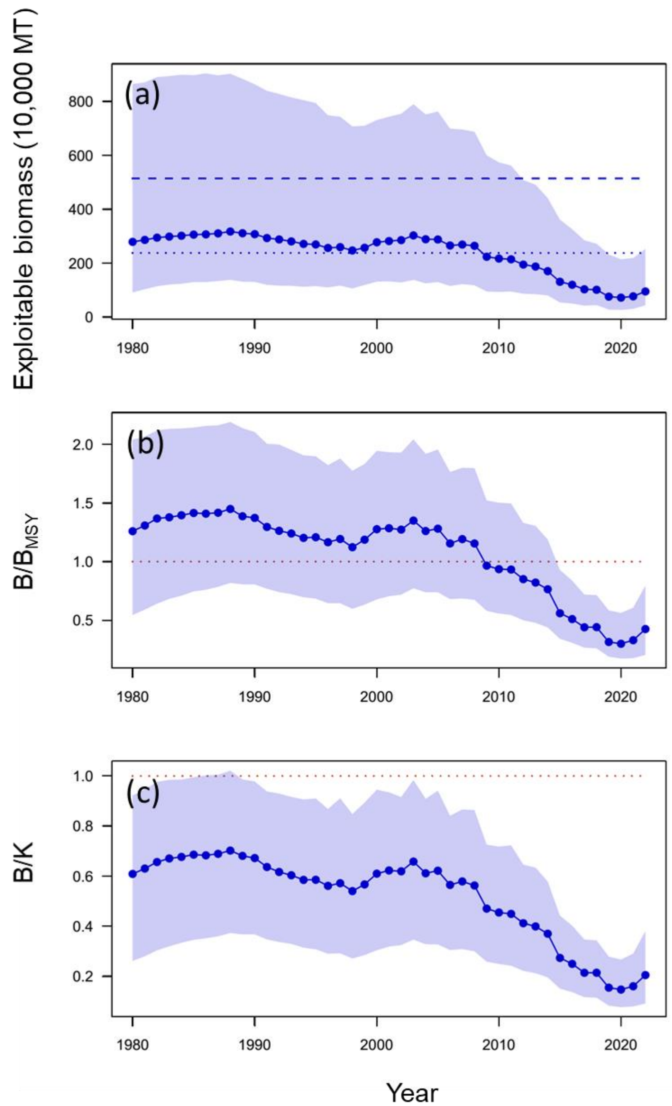

Figure S3. Time series of biomass (10,000 metric tons) (a), the ratio of biomass to B_{MSY} (B/B_{MSY}) (b), and depletion ratio (B/K) (c) of the western North Pacific saury for the base case 2. In panel (a), the upper dashed and lower dotted horizontal line denotes the carrying capacity (K) and B_{MSY}, respectively. In panels (b) and (c), the dashed lines denote the reference levels of 1.

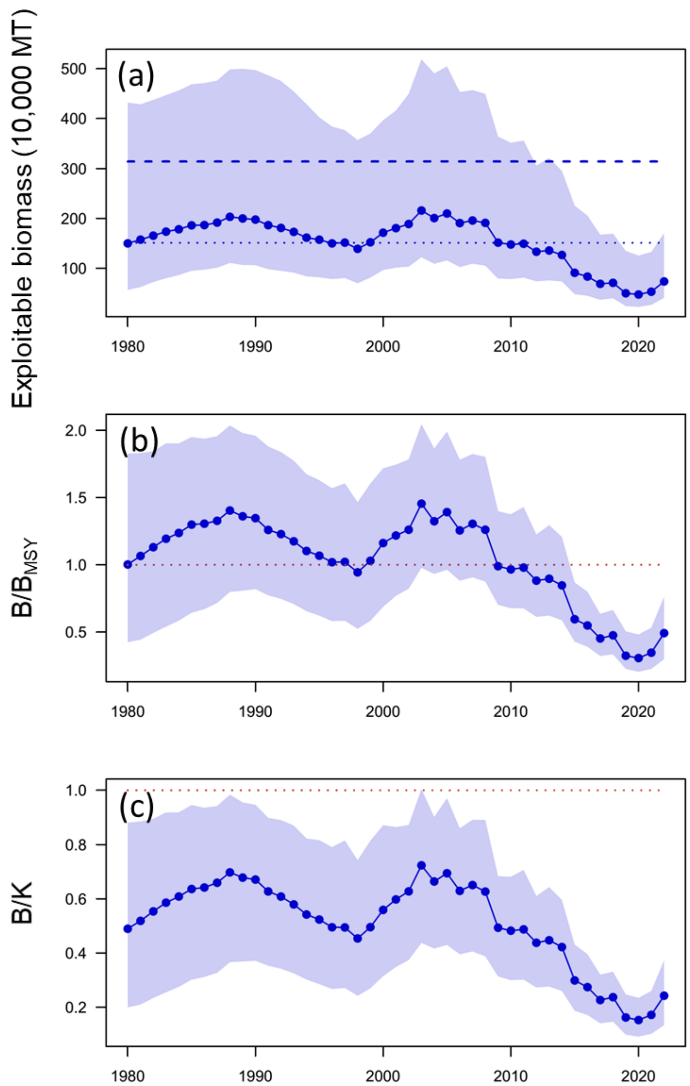

Figure S4. Time series of biomass (10,000 metric tons) (a), the ratio of biomass to B_{MSY} (B/B_{MSY}) (b), and depletion ratio (B/K) (c) of the western North Pacific saury for the sensitivity case 1. In panel (a), the upper dashed and lower dotted horizontal line denotes the carrying capacity (K) and B_{MSY}, respectively. In panels (b) and (c), the dashed lines denote the reference levels of 1.

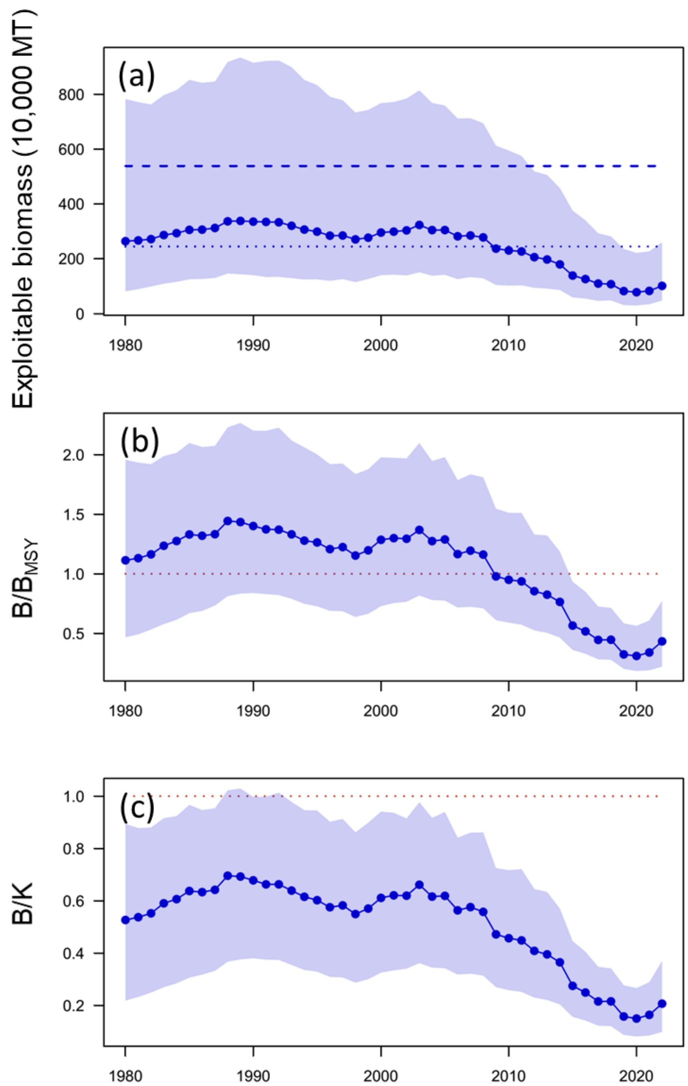

Figure S5. Time series of biomass (10,000 metric tons) (a), the ratio of biomass to B_{MSY} (B/B_{MSY}) (b), and depletion ratio (B/K) (c) of the western North Pacific saury for the sensitivity case 2. In panel (a), the upper dashed and lower dotted horizontal line denotes the carrying capacity (K) and B_{MSY}, respectively. In panels (b) and (c), the dashed lines denote the reference levels of 1.

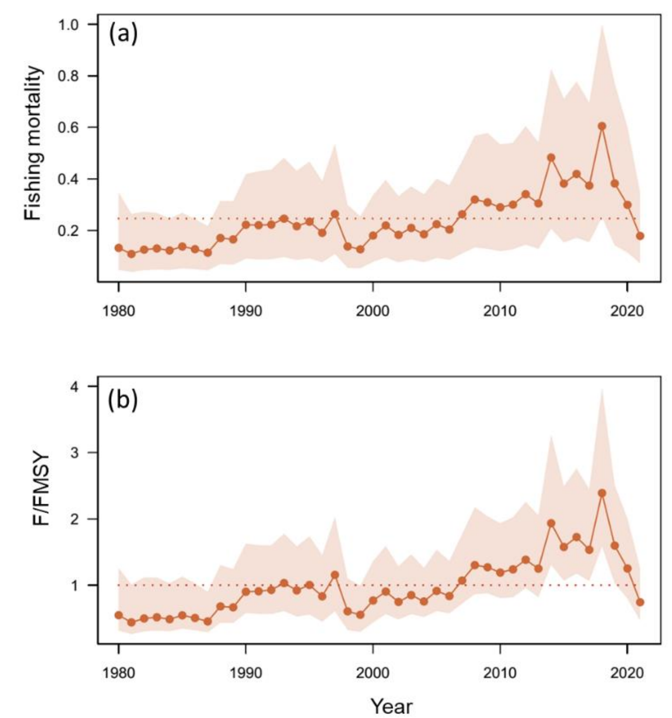

Figure S6. Time series of fishing mortality (a) and the ratio of fishing mortality to F_{MSY} (F/F_{MSY}) (b) of the Western North Pacific saury for the base case 1. In panel (a), the dashed line denotes the F_{MSY}. In panel (b), the dashed line denotes the reference levels of 1.

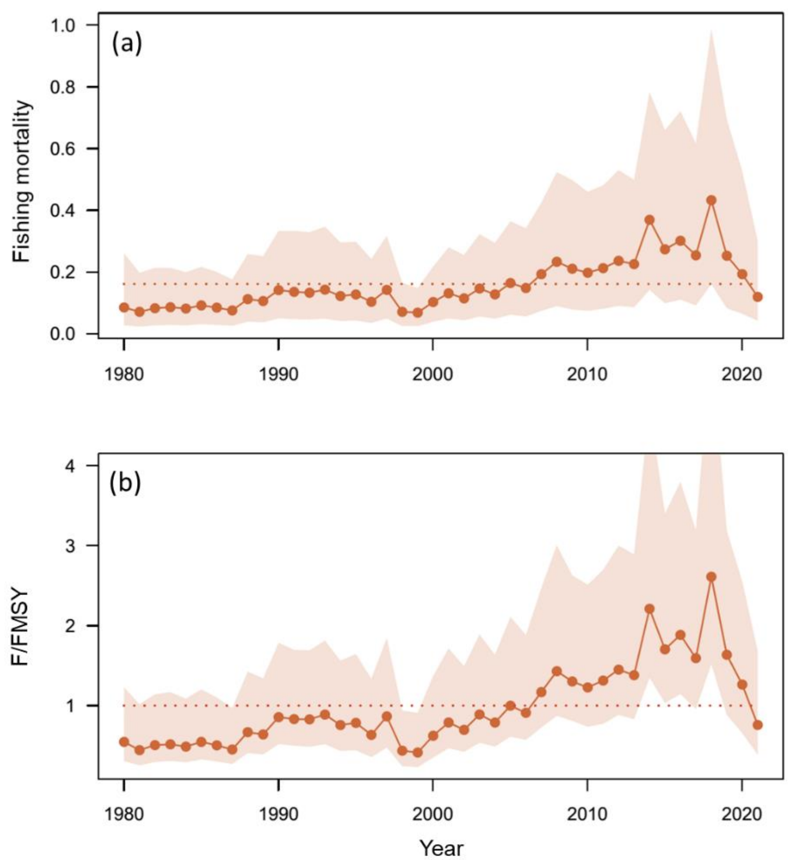

Figure S7. Time series of fishing mortality (a) and the ratio of fishing mortality to F_{MSY} (F/F_{MSY}) (b) of the Western North Pacific saury for the base case 2. In panel (a), the dashed line denotes the F_{MSY}. In panel (b), the dashed line denotes the reference levels of 1.

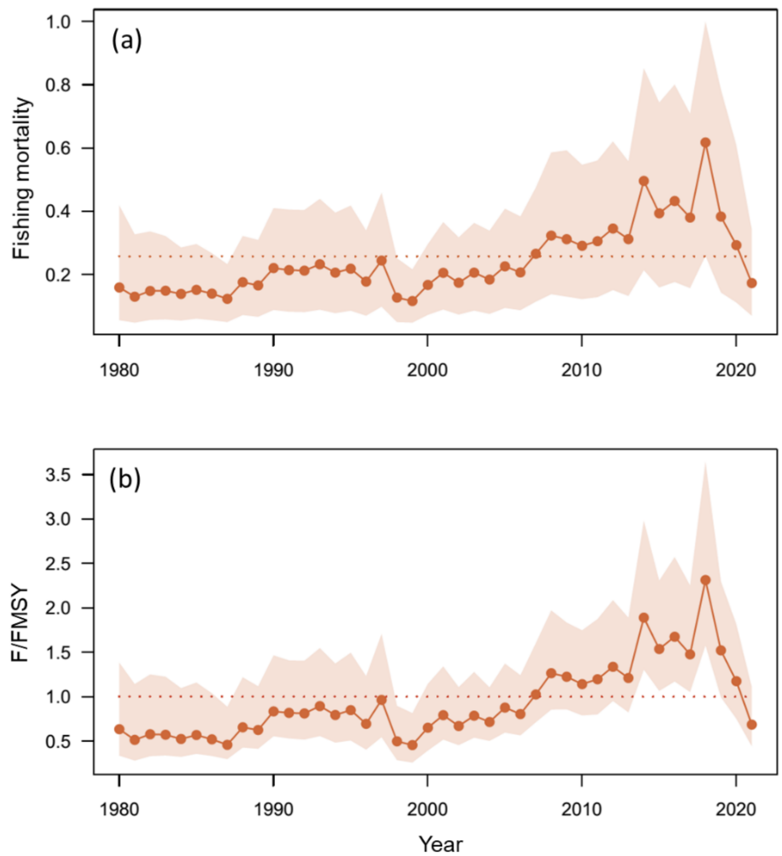

Figure S8. Time series of fishing mortality (a) and the ratio of fishing mortality to F_{MSY} (F/F_{MSY}) (b) of the Western North Pacific saury for the sensitivity case 1. In panel (a), the dashed line denotes the F_{MSY}. In panel (b), the dashed line denotes the reference levels of 1.

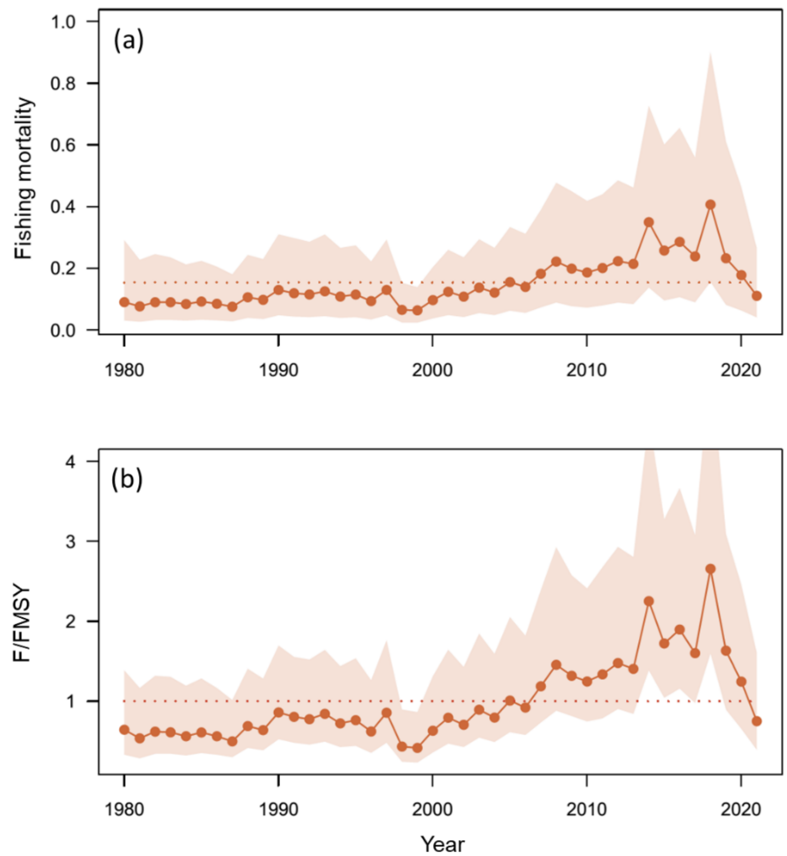

Figure S9. Time series of fishing mortality (a) and ratio of fishing mortality to F_{MSY} (F/F_{MSY}) (b) of the Western North Pacific saury for the sensitivity case 2. In panel (a), the dashed line denotes the F_{MSY}. In panel (b), the dashed line denotes the reference levels of 1.